Higher-order topological superconductor on the bipartite triangular lattice

A. D. Fedoseev *

Kirensky Institute of Physics, Federal Research Center KSC SB RAS, 660036 Krasnoyarsk, Russia

(Received 21 January 2022; revised 20 April 2022; accepted 22 April 2022; published 29 April 2022)

In order to investigate the possibility of construction of the higher-order topological superconductor on the triangular lattice, the different types of the coupling of chiral topological superconductor edge states are considered. It is demonstrated that the widespread criterion of the topological corner mode's appearance consisting in edge-state effective mass changing at the corner has to be modified in the case of multiple Dirac points in the edge-state spectrum. It is shown that the effective mass must be of the same sign at all Dirac points on one edge adjacent to the corner and be opposite at all the Dirac points on another one. For a two-dimensional system constructed from two chiral topological superconductors on the triangular lattice with inverted bands, two types of interactions leading to the higher-order topological superconducting phase are revealed.

DOI: 10.1103/PhysRevB.105.155423

I. INTRODUCTION

Recently, a novel class of nontrivial topological systems named higher-order topological insulators (HOTI) was proposed [1]. Both bulk and conventional (first-order) edge-fermion spectra of such systems are gapped, while gapless excitations on the surfaces and defects of codimension higher than one appear. It should be noted that the edge states arising on the domain walls between the regions with different topological numbers on the surface of the system (the second-order edge states) were investigated earlier in [2–5]. The proposed conception of higher-order topology was shortly applied to superconducting [6–11], photonic [12,13], acoustic [14–16], spintronic [17,18], and topoelectric systems [19–21].

The particular interest to topological systems of higher order is connected with the higher-order topological superconductors (HOTSC) according to the possibility of the Majorana modes' (MMs) implementation. The MMs are supposed to be of great significance for the topological quantum computations [22]. The proposed earlier one-dimensional (1D) systems providing MMs at their ends have several problems. It is difficult to form a purely 1D system and, additionally, any thickening of a nanowire leads to the broadening of the edge excitations along this thickening. As a result, the Majorana-type character of the system gives place to the chiral one [23,24]. Additionally, while the gapless excitation is still well separated from the bulk excitations, other edge excitations appear at the end of the wire and not so well separated from the zero-energy excitations. Two-dimensional (2D) HOTSC solves these problems since gapless excitations are localized directly at the corners of the system and separated from both bulk and conventional edge excitations by the gap.

The practical interest in HOTSC is connected with the braiding of MMs. The braiding procedure in topological superconductors (of any order) implies the spatial exchange of two MMs with continuous changing of system energy parameters, which leads to the phase shift of the ground-state wave function [25,26]. This procedure can only be done in the 2D system [22] and demands the MMs to be well localized and separated from the other excitations (see supplementary information of [26]). While one needs to construct different combinations of 1D wires [27–29] to achieve the first requirement, it is satisfied in 2D HOTSC by definition. The second requirement also can be satisfied in these systems. By now, several models of HOTSC of different complications providing braiding procedure have been proposed [30–32].

Most of the investigations devoted to the HOTIs and HOTSCs were carried out on the square lattice (for example [33–39]). One can find several studies of the honeycomb lattice [40–42], but there are few investigations of the corner excitations on the triangular lattice. The widespread way to construct the HOTI/HOTSC [6,7,10,11,31,32,43,44] is to take a conventional topological system and add a perturbation, which mixes the edge excitations and creates a gap in the edge spectrum of the system. Along with that, the effective (Dirac) mass of the edge excitations must be of a different sign for two adjacent edges. In such a way, the corner between these edges becomes a domain wall, and gapless excitation located at this corner appears in the way similar to the appearance of gapless excitation on the boundary between two conventional topological insulators with different topological number. Such topological corner excitations can appear and annihilate only in pairs [45] and consequently contradict the C_3 symmetry of the triangle-shaped systems on the triangular lattice.

The different approach to construct the HOTI was proposed, for example, on the kagome lattice [14,46–48]. Similarly to the Su-Schrieffer-Heeger chain model [49] the proposed method considers the special limit in which the corner sites of the triangular-shaped kagome lattice become decoupled and provide the gapless corner states. These states remain in the wide range of parameters outside the decoupled limit unless the edge spectrum gap closes. Unfortunately, this method can not be applied to create corner excitations in

*fad@iph.krasn.ru

the superconducting systems as one of its features on the triangular lattice is the absence of particle-hole symmetry. In addition, the topological nature of these corner excitations was argued recently [50]. Moreover, recent investigations suppose the topological corner excitations to be forbidden in the C_3-symmetric systems [51,52]. Meanwhile, the nontopological corner excitations in the C_3-symmetric superconducting system [53] and other manifestations of nontrivial topology such as charge anomaly [54] are still possible.

Although a number of different models of HOTSC were proposed, none of them have been found. The only one experimentally confirmed material providing the higher-order topology is bismuth [55,56]; however, some uncertainty still remains regarding the possibility of the observed effects to be the manifestation of the first-order topology [57]. Another HOTI candidate is transition-metal dichalcogenides [58–60], but there are still no experimental evidences for them to our knowledge. In spite of the weak success in experimental confirmation of higher-order topology in electronic systems, the profit of the 2D HOTSCs is great enough to continue searching for them. In addition the experimental confirmations of higher-order topology in photonic [12,13], acoustic [14–16] and topoelectrical [19–21] systems provide the prospect that such search will become more successful.

Taking the above into account, we investigate the possibility of construction of a HOTSC on the triangular lattice. Starting from the chiral topological superconductor on the triangular lattice we study the effect of different couplings on the edge spectrum and demonstrate which coupling can provide topological corner excitations in the system.

II. BIPARTITE TRIANGULAR SUPERCONDUCTING SYSTEM

We start our investigation with the chiral $(d+id)$-wave superconductor on the triangular lattice with the Hamiltonian

$$\mathcal{H} = (\Delta\varepsilon - \mu)\sum_{f\sigma} c^\dagger_{f\sigma}c_{f\sigma} + t\sum_{\langle fm\rangle\sigma} c^\dagger_{f\sigma}c_{m\sigma} + \sum_{\langle fm\rangle}(\Delta_{fm}c^\dagger_{f\uparrow}c^\dagger_{m\downarrow} + \text{H.c.}). \quad (1)$$

Here, f and m numerate the lattice sites, $\langle fm\rangle$ is summation over the nearest neighbors; μ is the chemical potential; $\Delta\varepsilon$ is onsite energy; $c^\dagger_{f\sigma}$ is the creation operator of the electron. We consider the case of superconducting order parameter, which couples electrons on the nearest neighbors and corresponds to the triangular lattice symmetry [Fig. 1(a)]:

$$\Delta_{fm} = \Delta_j = \Delta_1 e^{2\pi i(j-1)/3}, \quad j = 1,2,3. \quad (2)$$

The investigated system is a topological superconductor in the range $-3 < \mu/t < 6$ with the Chern number $C = 2$ [61,62] same for both spin projections σ. Most of the early HOTSCs investigations start with the conventional topological system with gapless edge states possessing only one Dirac point at high-symmetry point. Contrary to that, the current system provides two branches of gapless edge excitations at the boundary with Dirac points $\pm p_0$ both propagating in one direction resulting in $C = 2$ (see Appendix A for details).

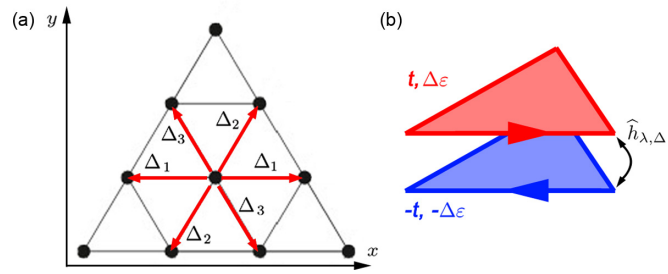

FIG. 1. (a) Directions of superconducting coupling Δ_j (2) for the chiral $(d+id)$-wave superconductivity on the triangular lattice. (b) Heterostructure combined from two topological superconductors with inverted bands. In the uncoupled regime, topological superconductors contain gapless edge states propagating in the opposite directions. These states are gapped with the $h_{\Delta,\lambda}$ interactions (3).

Below we will show that this feature is of great significance for the construction of the HOTSC.

As energy spectrum of edge excitations is the same for both spin projections, the addition of any couplings of relatively small values can not open the gap in the edge spectrum and consequently can not provide HOTSC. For example, magnetic field will result in splitting of the Dirac points in two pairs of points. So, if one needs to obtain the gapped edge spectrum it is necessary to add to the investigated system another system with inverted spectrum. It means that a bipartite triangle lattice should be taken in consideration with hopping amplitude and onsite energies having opposite signs for different sublattices and chemical potential $\mu = 0$ corresponding to overall half-filling. The visual representation is a heterostructure of two chiral topological superconductors [Fig. 1(b)].

The additional system with inverted spectrum is also a topological superconductor, but it is characterized with the Chern number of opposite sign $C = -2$. Both systems separately possess particle-hole symmetry with particle-hole operator squared to -1 and broken time-reversal symmetry thus belonging to the C class of the tenfold classification [63,64]. In spite of that, the combined system possesses the time-reversal symmetry (the similar situation was described in [62]), but in the absence of interband coupling the specific form of time-reversal operator can be different and, consequently, the class (CI or CII) can not be determined. This specific form and topological class depend on the form of inter-band coupling.

Now, we introduce a coupling between the sublattices with inverted bands. For simplicity, we take into account only coupling which does not mix fermions with different quasimomentum k. We start with the interactions, which couples fermions with only the same spin projections $\sigma' = \sigma$ or only with opposite spin projections $\sigma' = -\sigma$ in different lattices:

$$\mathcal{H}_{ex} = \sum_{k\sigma}[h_\lambda(k,\sigma)c^\dagger_{k\sigma}d_{k\sigma'} + h^*_\lambda(k,\sigma)d^\dagger_{k\sigma'}c_{k\sigma} + h_\Delta(k,\sigma)c^\dagger_{k\sigma}d^\dagger_{-k\bar{\sigma}'} + h^*_\Delta(k,\sigma)d_{-k\bar{\sigma}'}c_{k\sigma}]. \quad (3)$$

Here, the absence of the summation over σ' reflects that it is directly determined with σ, h_Δ refers to the superconducting coupling, h_λ corresponds to the hybridization processes, and

$d^{\dagger}_{k\sigma}$ is an electron creation operator in the topological superconductor with inverted band.

One of the differences between conventional topological insulators and superconductors and HOTI/HOTSC consists in the fact that higher-order topology is not necessarily connected with some bulk topological invariant. Topological corner modes can appear or vanish without closing of the bulk gap and the topological phase transition is connected with the edge-state spectrum closing (example given in [31,43,45,65]). Therefore, in order to investigate the possibility of higher-order superconducting topological phase in the proposed system, we will not calculate bulk invariants, but use the widespread effective mass sign criterion instead.

To analyze the possibility of implementation of the higher-order topological phase in the system, the Bogoliubov–de Gennes Hamiltonian is written and projected to the edge states (as they are the low-energy states of the system) at the boundary. The resulting effective Hamiltonian can be expressed in the following form (see Appendix B for details):

$$H_{\text{eff}} = \begin{bmatrix} \varepsilon_p & V \\ V^* & -\varepsilon_p \end{bmatrix},$$
$$V = \psi^*(x')\psi^*(y')[u^*_+u_-\widehat{h}_\lambda(k,\sigma) - v^*_+v_-\widehat{h}^*_\lambda(-k,\overline{\sigma}) + u^*_+v_-\widehat{h}_\Delta(k,\sigma) - v^*_+u_-\widehat{h}^*_\Delta(-k,\overline{\sigma})]\psi(x')\psi(y'), \quad (4)$$

where $\pm\varepsilon_p$ are the edge-state energies with quasimomentum p along the edge in different bands, u and v are the vector components of the edge-state wave functions along with index $\pm$ corresponding to different bands, $\psi(x')$, $\psi(y')$ are wave-function components depending on coordinates perpendicular and along the boundary, correspondingly, and the notating $(\psi^*(x')\psi^*(y')\widehat{h}_{\lambda,\Delta}(k,\sigma)\psi(x')\psi(y'))$ means integration over x', y' with $k \to -i\nabla$ substitution.

To obtain the topological corner states one needs the effective interaction V to change sign with changing of boundary orientation, defined with the angle ϕ between the perpendicular to the edge and x direction. The dependence on ϕ can be generated by the form of the h_Δ and h_λ interactions, or by the u^*v, v^*u terms in the component, containing h_Δ. So, as an example, we start with the constant superconducting triplet coupling with order parameter Δ_{ex}:

$$\mathcal{H}_{ex} = \Delta_{ex}\sum_{k\sigma}[c^{\dagger}_{k\sigma}d^{\dagger}_{-k\sigma} + d_{-k\sigma}c_{k\sigma}].$$

In such case, the dependence of V on edge orientation ϕ comes from u and v terms, and the effective mass at the Dirac points $\pm p_0$ has the form (see Appendix B for details)

$$m_{\text{eff}}(\pm p_0) = \pm\frac{\sigma m}{\sqrt{\Delta^2+m^2}}\Delta_{ex}\sin(2\phi+\theta_\Sigma/2),$$
$$m = 3t/2, \quad \Delta = 3|\Delta_1|/4,$$
$$\Delta^{\pm}_1 = |\Delta_1|e^{i\theta_\pm}, \ \theta_\Sigma = \theta_+ + \theta_-. \quad (5)$$

Here, $\theta_\pm$ are $(d+id)$-wave superconducting coupling parameter phase factors in different bands.

The obtained effective mass changes signs with changing of ϕ, but also it has different signs in different Dirac points at the same edge. Numerical calculations show that this form of coupling does not provide topological corner states although it provides gapless edge states at the predicted directions of the boundary. It becomes clear that for realization of the topological corner states it is necessary to have the effective mass of the edge states to be the same sign at both Dirac points. To achieve this goal, the superconducting coupling odd in k is necessary.

III. HOTSC FROM TWO CHIRAL TSC THROUGH THE SUPERCONDUCTING COUPLING

The only coupling that can satisfy the conditions of generation edge states' effective mass, which has the same sign at both Dirac points and changes sign with changing ϕ is the p-wave coupling (see Appendix B for details). Moreover, it must have a 1D representation. While such superconducting coupling is not realistic it is still useful to demonstrate clearly the appearance conditions of topological corner states in the investigated system.

Taking into account the p_x-wave superconducting coupling, one can easily obtain the effective mass

$$m_{\text{eff}}(\pm p_0) \sim \Delta_{ex}\sin\phi\ \sin(2\phi+\theta_\Sigma/2). \quad (6)$$

The obtained effective mass is the same at both Dirac points and changes its sign at six values of ϕ. The values $\phi = 0$ and π reflect the chosen direction of the coupling and can be changed with rotation of this direction. The other four values can be changed with changing of sum of chiral superconducting phase factors $\theta_\Sigma = \theta_+ + \theta_-$.

The described system possesses particle-hole and time-reversal symmetries both squared to -1, thus, it belongs to the *CII* class of tenfold classification. Also, it possesses the inversion symmetry with inversion operator, which commutates with particle-hole symmetry and anticommutates with time-reversal symmetry actions. Thus, the described system falls into the *CII* $(-+)$ class of higher-order topological systems protected with inversion symmetry [66].

As long as we have the same effective masses at both Dirac points and demand the effective interaction V dependence on ϕ to have the 1D representation, the sign of this mass becomes an edge topological invariant. Indeed, this sign has only two discrete values (which are determined up to simultaneous change of the signs at all edges), it is well defined when the edge spectrum gap is open, and it cannot be changed without closing of this gap. So, we have a combination of three edge invariants, which determine the topological properties of our system. The system is trivial if effective masses at all edges have the same sign, and it is in the higher-order topological phase if the sign of effective mass is different at different edges, providing the gapless corner modes at the corners between the edges with different signs of effective masses.

To describe the appearance of the corner modes, it is useful to illustrate the values of ϕ at which the effective mass sign changes, as points at the circle corresponding to the ϕ interval (Fig. 2). To understand whether a topological state occurs at some corner on the open boundary, one should put additional points on this circle corresponding to the orientation of the perpendiculars to the edges, adjacent to the investigated corner and count the number of mass sign-changing points between them. This procedure has a perfectly clear visual representation in the case of a triangle-shaped system

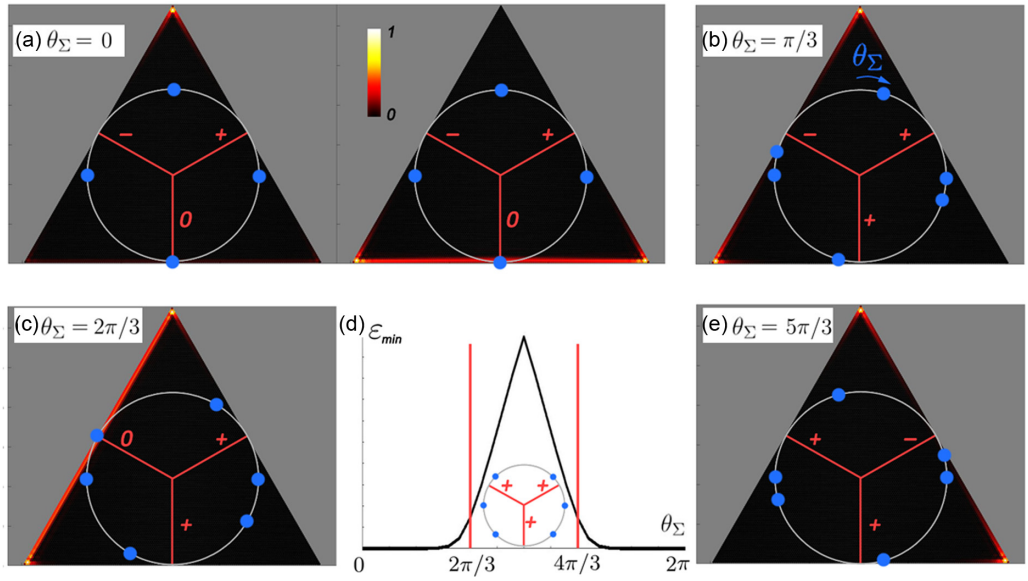

FIG. 2. Topological corner states in the triangle-shaped heterostructure of two topological superconductors with inverted bands, coupled with the p_x-wave superconducting coupling. (a) Normalized spatial distribution (summed for both sublattices) of gapless corner excitation (left) and gapless edge excitation (right) for $\theta_\Sigma = 0$ along with corresponding values of ϕ. Two pairs of points at $\phi = 0$ and π coincide. Lines denote perpendiculars to the triangle edges, $\pm$ denote signs of the effective masses at corresponding edges, 0 corresponds to gapless edge states at the edge. (b), (c), (e) Gapless corner and edge excitations for different values of θ_Σ. (d) Dependence of the energy of lowest excitation on θ_Σ. The energy spectrum is gapped at $2\pi/3 < \theta_\Sigma < 4\pi/3$ and gapless (up to the finite-size effects) otherwise.

(Fig. 2). In this case, one can draw a circle inscribed in the triangle-shaped border and put perpendiculars to the edges, which divide the circle into three sectors corresponding to three corners. If the sector contains an odd number of effective mass sign-changing points, the signs of the effective masses at the adjacent edges are different and the corresponding corner provides the gapless topological corner mode. If the number is even, there is no topological corner mode (while there still can be a nontopological gapped mode).

Now, we demonstrate the comparison of introduced analytics with the numerical calculations (Fig. 2). In our case, at $\theta_\Sigma = 0$ there is one topological corner state along with a gapless mode on the opposite edge [Fig. 2(a)] similar to the case in [11] (the maxima of the edge-state spatial distribution at corners is due to tendency of the conventional edge states to localize at the corners in the limited systems [67]). With changing of θ_Σ we can move the group of four effective mass sign-changing points along the circle forcing them to cross the perpendiculars to the edges and consequently move the corner modes from one corner to another. At $0 < \theta_\Sigma < 2\pi/3$ [Fig. 2(b)] there are two corners with odd numbers of points in corresponding sectors providing topological corner modes on the left side of the triangle. At $\theta_\Sigma = 2\pi/3$, one of the points crosses the perpendicular to the left boundary of the triangle inducing a gapless edge state at it [Fig. 2(c)]. At $2\pi/3 < \theta_\Sigma < 4\pi/3$, there are even numbers of points at all sectors and, consequently, the topological states do not appear and the fermion spectrum is gapped [Fig. 2(d)]. At $4\pi/3 < \theta_\Sigma < 2\pi$, there are two gapless corner modes on the right side of the triangle [Fig. 2(e)].

While it was shown the theoretical possibility of topological corner modes' appearance on triangular lattice and even of moving them from corner to corner, these modes can not be used for braiding for several reasons. First, the introduced rotating procedure has an interval of θ_Σ at which topological corner states collapse. Second, along the procedure the edge-state spectrum closes several times, preventing the braiding procedure. Finally, the 1D representation of superconducting p-wave coupling is not realistic, whereas more realistic $(p + ip)$-wave coupling does not generate the effective mass sign-changing points. Nevertheless, the described case was a simple demonstration of how the HOTSC criterion works in the system with two Dirac points in the conventional edge spectrum.

IV. HOTSC FROM TWO CHIRAL TSC THROUGH HYBRIDIZATION

As the procedure of topological corner-state generation was clearly demonstrated on the case of superconducting coupling between the sublattices now we proceed to more realistic case of hybridization coupling. In this case, the form of the edge-state wave functions does not generate the dependence of V on boundary direction ϕ and, consequently, this dependence has to be generated with the coupling itself. Although the wave-function form in this case does not forbid the k odd-parity couplings, they appear not to generate effective mass changing in the system and, consequently, can not create a HOTSC. The only coupling appropriate for this task is again the p-wave coupling with additional conditions on the difference between chiral superconducting order phase factors $\delta\theta = \theta_+ - \theta_-$ (see Appendix B for details). The effective mass dependence on ϕ takes the form

$$m_{\text{eff}}(\pm p_0) \sim \sin(\phi - \phi_{ex}), \tag{7}$$

where ϕ_{ex} correspond to the coupling direction.

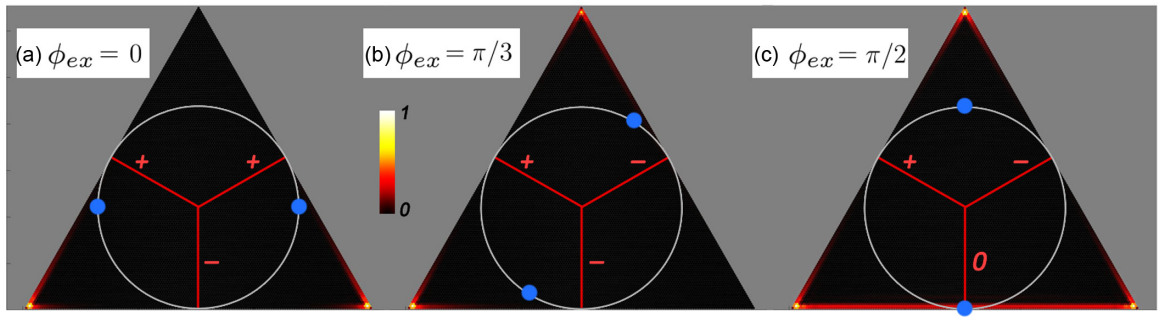

FIG. 3. Topological gapless states in the triangle-shaped heterostructure of two topological superconductors with inverted bands, coupled with Rashba-type interband spin-orbital interaction. Color field depicts spatial distributions of normalized amplitude of the gapless states for different directions of coupling ϕ_{ex}, points at the circle mark values of angle ϕ, at which the effective mass changes sign. Lines denote perpendiculars to the triangle edges, $\pm$ denote signs of the effective masses at corresponding edges, and 0 corresponds to gapless edge states at the edge. (a), (b) Gapless corner modes. (c) Gapless corner mode combined with gapless edge mode.

In this case, there are only two effective mass sign-changing points, generated by the coupling. In the way similar to described earlier, the hybridization provides a pair of gapless corner modes or a corner mode and gapless edge mode in the triangle-shaped system conditionally on the relative direction of coupling and boundaries (Fig. 3). Contrary to the previous case, the position of the gapless modes is controlled only by the direction of the coupling ϕ_{ex} and can not be changed by other parameters of the system. On the other hand, the additional advantage of using hybridization consists in the fact that it always generates two gapless modes independently on its direction. Nevertheless, it can not be used for braiding since it still closes the edge-state gap at several directions.

Although in this case the system is less flexible and less clear for demonstration, it seems to be more realistic since the hybridization is allowed to be of the Rashba spin-orbit coupling form. The direction of the field controls the direction of the interband coupling. In this case the difference of chiral superconducting phases factors in different bands has to be $\delta\theta = \pi$ (see Appendix B). The system under consideration again falls into the *CII* $(-+)$ class [66] as it was in the case of superconducing coupling examined previously, providing topological corner excitations.

V. TWO-LAYERED SYSTEM WITH MAGNETIC FIELD

The research described above examined the interactions, which couple the edge states of two chiral topological superconductors pairwise, allowing us to divide the space into two subspaces. Taking into account magnetic field (or another type of interaction mixing both edge states of one superconductor) forces us to deal with all four edge states, much complicating the analysis. Still, some conclusions can be made. In Sec. II, we discussed that the magnetic field itself can not open a gap in the conventional edge spectrum of the chiral topological superconductor on the triangular lattice. However, the prospects of its application to the investigated heterostructure need to be studied. The aim is to understand whether the magnetic field can simplify the form of coupling required for HOTSC creation.

The mathematical details of investigation can be found in Appendix C. The k-independent interband interactions can not generate topological corner states because of the same reasons, which were discussed earlier. Meanwhile, the situation with the coupling proportional to k^2 (d coupling or extended s coupling) changes. In the absence of magnetic field, such kind of coupling does not generate the ϕ dependence of the effective mass at Dirac points and, consequently, can not create topological corner states. In the presence of magnetic field both Dirac points are split into pairs, and there can appear a dependence proportional to $\cos(2\phi)$. Moreover, in the case of hybridization, the effective mass is independent of p sign. Unfortunately, it is of opposite signs in the split Dirac points in every pair providing no gapless corner modes in the system.

VI. CONCLUSION

The possibility of creation of HOTSC based on 2D chiral topological superconductors on the triangular lattice was demonstrated. It was shown that a bipartite lattice containing two topological superconductors with inverted bands is required. To achieve the goal, different types of couplings between these superconductors were examined. On the example of such a system it was shown that the widespread criterion of topological corner-mode appearance has to be modified in the case of multiple Dirac points in the edge spectrum. In this case, the requirement of changing sign of effective mass at the corner is accompanied by the requirement of the effective mass sign to be the same at both Dirac points at one boundary. It was shown that only the p-wave superconducting and hybridization coupling can generate a HOTSC phase in the investigated system. The analysis was confirmed with numerical calculations of the fermion excitation spectrum and their spatial distribution in the system with triangle-shaped boundary. The latter showed the appearance of gapless corner modes in full agreement with analytical predictions.

ACKNOWLEDGMENTS

The author thanks M. M. Korovushkin, S. V. Aksenov, M. S. Shustin, V. A. Mitskan, A. O. Zlotnikov, and D. M. Dzebisashvili for the fruitful discussions and valuable remarks. The reported study was funded by the Russian Foundation for Basic Research, Government of Krasnoyarsk Territory, Krasnoyarsk Regional Fund of Science to the research projects:

"Study of edge states in one- and two-dimensional topological superconductors" (Grant No. 20-42-243005).

APPENDIX A: WAVE FUNCTIONS AND SPECTRUM OF THE EDGE STATES IN THE TOPOLOGICAL CHIRAL SUPERCONDUCTOR ON TRIANGULAR LATTICE

Let us consider the system described by the Hamiltonian (1). To obtain the edge-state spectrum and wave functions of the system we follow the procedure, well described in [7,31]. At first, we write the Bogoliubov–de Gennes Hamiltonian in the basis $(c_{k\sigma}, c^{\dagger}_{k\bar{\sigma}})$:

$$H = \begin{bmatrix} t_k + \Delta\varepsilon - \mu & \sigma\Delta_k^* \\ \sigma\Delta_k & -(t_k + \Delta\varepsilon - \mu) \end{bmatrix},$$
$$t_k = 2t\left(\cos k_x + 2\cos\frac{k_x}{2}\cos\frac{k_y\sqrt{3}}{2}\right),$$
$$\Delta_k = 2\Delta_1\left(\cos k_x - \cos\frac{k_x}{2}\cos\frac{k_y\sqrt{3}}{2}\right) - 2i\sqrt{3}\Delta_1\sin\frac{k_x}{2}\sin\frac{k_y\sqrt{3}}{2}. \quad \text{(A1)}$$

The edge states in cylinder geometry (open boundary conditions in one direction and periodical in other one) appear in the vicinity of points, at which the bulk spectrum gap closes at topological phase transition. As in our case, the $(d + id)$-wave superconducting coupling has a 2D representation, the gap closure occurs at nodal points of Δ_k. While it has two nodal points, at the center of the Brillouin zone and at its corner [68], for simplicity we consider the chemical potential to be close to the value of $t_k + \Delta\varepsilon$ at $k = (0, 0)$. Using the low-energy continued limit, introducing the substitution $(k_x, k_y) = -i(\partial_x, \partial_y)$ and using the local coordinates of the boundary, the Bogoliubov–de Gennes Hamiltonian will take the form

$$H = \begin{bmatrix} m_0 + m\left(\partial_{x'}^2 + \partial_{y'}^2\right) & -\sigma\Delta_\phi(\partial_{y'} - i\partial_{x'})^2 \\ -\sigma\Delta_\phi^*(\partial_{y'} + i\partial_{x'})^2 & -m_0 - m\left(\partial_{x'}^2 + \partial_{y'}^2\right) \end{bmatrix},$$
$$m_0 = 6t + \Delta\varepsilon - \mu, \quad m = 3t/2, \quad \Delta_\phi = \Delta e^{2i\phi + i\theta},$$
$$\Delta = 3|\Delta_1|/4, \quad \Delta_1 = |\Delta_1|e^{i\theta}. \quad \text{(A2)}$$

Here, the y' axis is directed along the open boundary and x' is perpendicular to the boundary and points outside the system; ϕ is an angle between x and x' axis (Fig. 4).

The solution of the Schrödinger equation $H\Psi = \varepsilon\Psi$ with open boundary conditions $\Psi(x' = 0, y') = 0$ has the form (Fig. 5)

$$\varepsilon_p = -\Delta\,\mathrm{sign}(p)\frac{m_0 - 2mp^2}{\widetilde{m}^2}, \quad \widetilde{m} = \sqrt{\Delta^2 + m^2},$$
$$\Psi(x', y') = \frac{1}{\sqrt{|u|^2 + |v|^2}}\begin{bmatrix} u \\ v \end{bmatrix}\psi(x')\psi(y'),$$
$$\psi(x') = \frac{1}{\sqrt{\mathcal{N}_x}}\sin(\mathrm{Im}\lambda x')e^{\mathrm{Re}\lambda x'}, \quad \psi(y') = \frac{e^{ipy'}}{\sqrt{\mathcal{N}_y}},$$
$$\lambda = \frac{1}{\widetilde{m}}[\Delta|p| + i\sqrt{m(m_0 - mp^2)}],$$

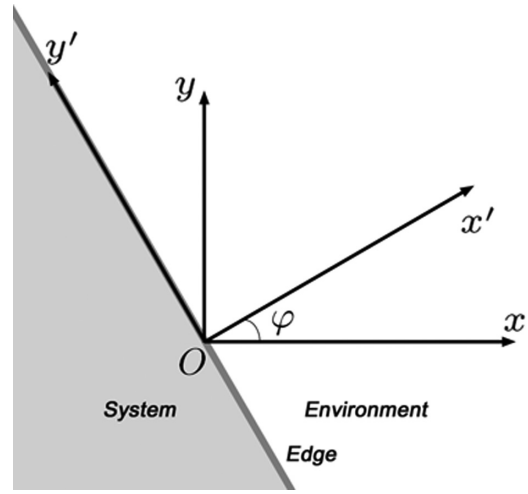

FIG. 4. Boundary of the system with arbitrary direction. Local coordinates are directed along (y') and perpendicular (x') to the edge.

$$u = -\sigma\Delta_\phi(p - \lambda)^2A^*, \quad v = |A|^2,$$
$$A = [m_0\Delta^2 + \mathrm{sign}(p)\Delta(m_0 - 2mp^2)\widetilde{m} + 2i\Delta m|p|\sqrt{m(m_0 - mp^2)}]/\widetilde{m}^2, \quad \text{(A3)}$$

Here, p is quasimomentum along the boundary, value $(p - \lambda)^2A^*$ appears to be real, and $\mathcal{N}_x, \mathcal{N}_y$ are normalization factors of the coordinate part of the wave function:

$$\mathcal{N}_x = \int_{-\infty}^{0} dx' \sin^2(\mathrm{Im}\lambda_1 x')e^{2\mathrm{Re}\lambda_1 x'}, \quad \mathcal{N}_y = \int_{-\infty}^{\infty} dy'.$$

The obtained solution is appropriate for $0 < |p| < m_0/m$. They are doubly degenerated according to $\sigma = \pm 1$, spread along the edge in one direction for both branches ($p > 0$ and $p < 0$), and have no counterpart with opposite sign $-\varepsilon_p$ at the

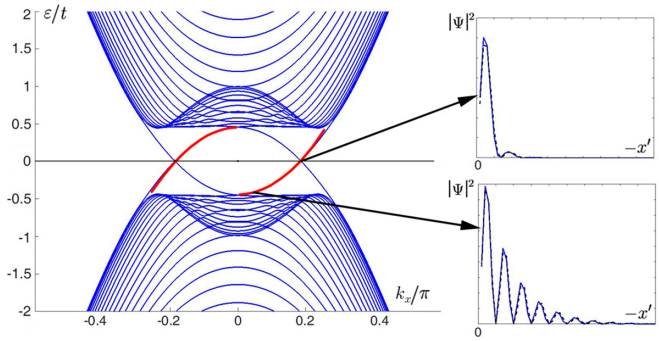

FIG. 5. Left: Spectrum of the chiral topological superconductor on the triangular lattice in the cylinder geometry. Blue lines denote result of the numerical calculations for system with two boundaries in the y direction and periodical boundary conditions in the x direction. Red lines mark the theoretical solutions (A3) with $\phi = -\pi/2$. The inverted branches of the edge-state spectrum in numerical calculation are caused by the presence of two edges with $p = k_x$ for one edge and $p = -k_x$ for opposite. Right: Wave-function amplitude spatial distribution for p close to 0 and p close to the Dirac point p_0. Blue lines present the result of the numerical calculation, and dashed black line corresponds to the theoretical prediction (A3).

same p. Consequently, one can not construct a HOTSC by perturbation of this system since any small perturbation will not open the gap, and the gapless topological edge states remain. The position of the Dirac points in the edge spectrum $\pm p_0$ are parameter dependent $p_0 = \sqrt{m_0/2m}$. That is contrary to most of the earlier investigations of HOTSCs, in which there was only one Dirac point pinned to a high-symmetry point. One also can see that in our notation all wave-function dependence on the boundary direction ϕ and chiral order parameter phase θ is put in u.

As long as we are interested in the properties of the edge states around the Dirac points it is better to rewrite the spectrum and λ for more clarity:

$$\begin{aligned}\varepsilon_p &= -2s\frac{m\Delta}{\widetilde{m}}(p_0^2 - p^2),\\ \lambda &= \frac{1}{\widetilde{m}}[\Delta|p| + i|m|\sqrt{2p_0^2 - p^2}],\\ p_0 &= \sqrt{m_0/2m}, \quad s = \mathrm{sign}(p).\end{aligned} \tag{A4}$$

It is easy to notice that $|\lambda(\pm p_0)| = p_0$, which will be important further.

APPENDIX B: EFFECT OF PERTURBATION WITHOUT SPIN PROJECTION MIXING ON THE EDGE STATES

As analysis of the system with two effective bands is easier to understand, we start with the perturbation that couple the edge states with spin projection σ in one topological superconductor with either projection $\sigma' = \sigma$ or $\sigma' = -\sigma$ in the other, thus dividing the full basis of four edge states into two subspaces. Additionally, we will consider the perturbation, which couples only fermions with the same quasimomentum k:

$$\begin{aligned}\mathcal{H}_{ex} = \sum_{k\sigma}\big[&h_\lambda(k,\sigma)c^\dagger_{k\sigma}d_{k\sigma'} + h^*_\lambda(k,\sigma)d^\dagger_{k\sigma'}c_{k\sigma}\\ &+ h_\Delta(k,\sigma)c^\dagger_{k\sigma}d^\dagger_{-k\overline{\sigma'}} + h^*_\Delta(k,\sigma)d_{-k\overline{\sigma'}}c_{k\sigma}\big].\end{aligned} \tag{B1}$$

The Bogoliubov–de Gennes Hamiltonian of the perturbation in the basis $(c_{k\sigma}, c^\dagger_{-k\overline{\sigma}}, d_{k\sigma'}, d^\dagger_{-k\overline{\sigma'}})$ has the form

$$\begin{aligned}H_{ex} &= \begin{bmatrix}\mathbf{0} & H_{\mathrm{int}}\\ H^*_{\mathrm{int}} & \mathbf{0}\end{bmatrix},\\ H_{\mathrm{int}} &= \begin{bmatrix}h_\lambda(k,\sigma) & h_\Delta(k,\sigma)\\ -h^*_\Delta(-k,\overline{\sigma}) & -h^*_\lambda(-k,\overline{\sigma})\end{bmatrix},\end{aligned} \tag{B2}$$

where $\mathbf{0}$ is a 2×2 zero matrix.

We will refer to the edge states of topological superconductors as $|\pm,\sigma\rangle$, where $\pm$ denotes the edge states (A3) from different topological superconductors. We are mostly interested in the form of the edge-state coupling:

$$\begin{aligned}\langle +,\sigma|H_{ex}|-,\sigma'\rangle = \psi(x')\psi(y')^*[&u^*_+u_-\widehat{h}_\lambda(k,\sigma)\\ &- v^*_+v_-\widehat{h}^*_\lambda(-k,\overline{\sigma}) + u^*_+v_-\widehat{h}_\Delta(k,\sigma)\\ &- v^*_+u_-\widehat{h}^*_\Delta(-k,\overline{\sigma})]\psi(x')\psi(y')/(u^2{+}v^2).\end{aligned} \tag{B3}$$

Here, $(\psi(x')\psi^*(y')\widehat{h}_{\lambda,\Delta}(k,\sigma)\psi(x')\psi(y'))$ means integration over x', y' with $k\to -i\nabla$ substitution.

As we are interested in the effective mass at the Dirac points of the edge spectrum, it is useful to calculate the u, v products at these points:

$$\begin{aligned}\mathcal{N}_0 &= u^2 + v^2 = \frac{2\Delta^4 m_0^4}{m^2\widetilde{m}^2}\left[1 - s\frac{\Delta}{\widetilde{m}}\right],\\ u^2 &= \frac{1}{2}\left[1 - s\frac{\Delta}{\widetilde{m}}\right]\mathcal{N}_0, \quad v^2 = \frac{1}{2}\left[1 + s\frac{\Delta}{\widetilde{m}}\right]\mathcal{N}_0,\\ uv &= s\frac{m}{2\widetilde{m}}\mathcal{N}_0,\end{aligned} \tag{B4}$$

where u and v are taken from the same sublattice and $s = \mathrm{sign}(p)$ is a sign of quasimomentum along the edge at the Dirac point. Taking into account (B4) and noticing that $v_+ = v_-$, $u_+ = -\sigma\sigma' e^{i\delta\theta}u_-$ with $\delta\theta = \theta_+ - \theta_-$, the final form of (B3) we can obtain

$$\begin{aligned}&\langle +,\sigma|H_{ex}|-,\sigma'\rangle\\ &= -e^{i(\phi_\sigma+\phi_\lambda-\delta\theta)/2}(\psi(x')\psi^*(y')\widehat{h}_\lambda(k,\sigma)\psi(x')\psi(y'))\\ &\quad\times\left[\cos\left(\frac{\delta\theta-\phi_\sigma+\phi_\lambda}{2}\right)+\frac{is\Delta}{\widetilde{m}}\sin\left(\frac{\delta\theta-\phi_\sigma+\phi_\lambda}{2}\right)\right]\\ &\quad+\frac{s\sigma m}{\widetilde{m}}e^{i(\theta_\Sigma+\phi_\sigma+\phi_\Delta)/2}\cos\left(2\phi+\frac{\theta_\Sigma+\phi_\sigma+\phi_\Delta}{2}\right)\\ &\quad\times(\psi(x')\psi^*(y')\widehat{h}_\Delta(k,\sigma)\psi(x')\psi(y')),\\ &\delta\theta = \theta_+ - \theta_-, \quad \theta_\Sigma = \theta_+ + \theta_-,\\ &\phi_\sigma = (\sigma-\sigma')\pi/2, \quad h^*_{\lambda,\Delta}(-k,\overline{\sigma}) = e^{i\phi_{\lambda,\Delta}}h_{\lambda,\Delta}(k,\sigma).\end{aligned} \tag{B5}$$

Since $\widehat{h}_{\lambda,\Delta}$ with $k\to -i\nabla$ substitution are the combinations of differential operators ∂^n_x, ∂^n_y, we need the integrals

$$\begin{aligned}I_{yn} &= \int\psi^*(y')\partial^n_{y'}\psi(y')dy' = (ip)^n,\\ I_{xn} &= \int_{-\infty}^{0}\psi^*(x')\partial^n_{x'}\psi(x')dx' = -|\lambda|^n\frac{\mathrm{Im}\lambda^{n-1}}{\mathrm{Im}\lambda},\\ I_{x0} &= 1, \quad I_{x1} = 0, \quad I_{x2} = -|\lambda|^2, \quad I_{x3} = -2\,\mathrm{Re}\lambda|\lambda|^2.\end{aligned} \tag{B6}$$

Now we are ready to analyze the possibility of creation HOTSC by the combination of two topological superconductors with inverted bands. To obtain the topological corner states, the effective mass at the Dirac points has to change the sign with changing of boundary direction ϕ. It means that coupling (B5) must depend on ϕ and this dependence is forbidden to be complex. This coupling can be imagined as an effective field, splitting two levels. For the implementation of a clear inversion of the levels at the Dirac point, the value of this field should maintain its direction and change the sign with change of ϕ. So, any unremovable complexity in ϕ dependence is forbidden. This demand guarantees that we can introduce the signs of effective masses at the Dirac points (which are defined up to changing of signs at all edges simultaneously), which appears to be good edge topological invariants, as they are quantized and can change only with the closure of the edge-state spectrum gap.

Starting with the second item of (B5), which describes the interband superconducting coupling, as a more clear one,

one can notice that it already has a ϕ dependence and, moreover, the ϕ direction of boundary at which the effective mass changes sign can be smoothly controlled by the sum of the superconducting parameters θ_Σ. Unfortunately, it also has a factor of s, which leads to the opposite signs of the effective mass at the different Dirac points on one side for any perturbation even in k. For example, the case of triplet constant interband superconducting coupling, discussed in Sec. II, corresponds to $\sigma' = \overline{\sigma}$, $h_\Delta = \Delta_{ex}$, $\phi_\sigma = \sigma\pi$, $\phi_\Delta = 0$, and integrals to be equal to one. At Dirac points, this leads to the expression

$$\langle +, \sigma | H_{ex} | -, \overline{\sigma} \rangle = e^{i(\theta_\Sigma + \sigma\pi)/2} \Delta_{ex} \frac{s\sigma m}{\widetilde{m}} \sin\left(2\phi + \frac{\theta_\Sigma}{2}\right), \tag{B7}$$

where s is a sign of quasimomentum along the edge at the Dirac point. As the complex prefactor in (B7) does not depend on the orientation of the edge, it can be neglected, leading to the effective mass (5).

In the case of any superconducting coupling even in k, the topological corner modes do not appear because of the different effective mass signs in different Dirac points on the same edge. Consequently, it is necessary to take the coupling, which is odd in k to solve this problem. The p-wave coupling with $h_\Delta \sim k$ is a good choice. But, it is necessary to remember that it must not get a complex ϕ dependence in the x', y' coordinates. Consequently, $p + ip$ type is not appropriate as it generates a $e^{i\phi}$ factor.

The degrees of k more than two are also revealed to be useless for gapless corner-mode creation as in x', y' coordinates they provide a composition of integrals of real and imaginary values along with I_{xn} having different values for $n > 2$. Thus, they generate an unremovable complexity in ϕ dependence of edge-state coupling.

Now we proceed with the first term in (B5), which is caused by spin-preserved or spin-flip hybridization process. As we have seen on the example of superconducting coupling, the effective mass has to be of the same sign at both Dirac points on one boundary. So, it is necessary to remove the complexity in the brackets. It can be done in two ways. Removing the s-dependent part, one has to find h_λ, which is odd in k and generates noncomplex ϕ dependence. Unfortunately, there is none. The constant dependence is invariant under rotation of boundary. The second order in k coupling does not generate a ϕ dependence either because of the $I_{x2} = I_{y2}$ equality at the Dirac points $\pm p_0$. Couplings with order of k more than two generate unremovable complexity. So, this case does not provide any topological corner modes.

By removing the part in the brackets, which does not depend on s, one can obtain the situation similar to the situation with superconducting coupling discussed earlier. There are only two differences. First, the dependence on ϕ will be only generated with the perturbation. Taking $h_\lambda \sim (k_x \cos\phi_{ex} + k_y \sin\phi_{ex})$, where ϕ_{ex} corresponds to the coupling direction, one will straightforwardly obtain the effective mass $m_{\text{eff}} \sim \sin(\phi - \phi_{ex})$ with two points, at which effective mass changes sign. Second, these points are no longer controlled with the $\theta_\pm$ phases. The difference in these phases has to be set $\delta\theta = \pi + \phi_\sigma - \phi_\lambda$ to remove the s-independent term. For example, for Rashba-type coupling $h_\lambda \sim 2\sigma \sin k_x$ this difference has to be $\delta\theta = \pi$.

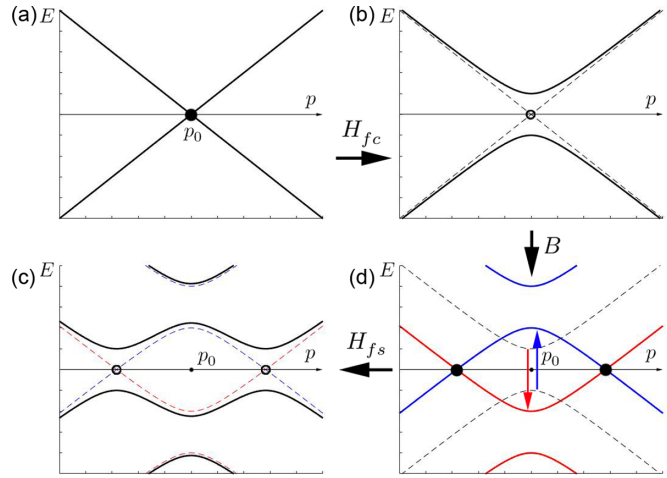

FIG. 6. Schematic depiction of the edge-spectrum modification of the 2D topological superconductor heterostructure with interband coupling (C2) in the vicinity of one of the Dirac points $\pm p_0$. Clockwise: (a) without coupling, (b) spectrum is gapped with H_{fc} term at Dirac point, (d) B removes the twofold degeneracy and shifts the spectrum creating two pairs of new Dirac points around p_0, (c) H_{fs} term gaps the spectrum at new Dirac points.

APPENDIX C: EFFECT OF PERTURBATION MIXING OF ALL FOUR EDGE STATES

Now it is desirable to understand whether the mixing of all four edge states can simplify the coupling form required for HOTSC creation from two topological superconductors with inverted bands. To avoid unnecessary overloading details, we start with the effective four-band Hamiltonian, obtained after projection of the perturbation on all four edge states in the system with a brief discussion of its component origin:

$$\Psi_{\text{basis}} = [|+,\uparrow\rangle|+,\downarrow\rangle|-,\uparrow\rangle|-,\downarrow\rangle]^T,$$
$$H = \begin{bmatrix} \varepsilon_p & H_c & H_{h\uparrow} & H_{f\uparrow} \\ H_c^* & \varepsilon_p & H_{f\downarrow} & H_{h\downarrow} \\ H_{h\uparrow}^* & H_{f\downarrow}^* & -\varepsilon_p & H_d \\ H_{f\uparrow}^* & H_{h\downarrow}^* & H_d^* & -\varepsilon_p \end{bmatrix}. \tag{C1}$$

Here H_c and H_d arise from intraband spin-mixing coupling in topological superconductors (such as magnetic field and spin-orbit interaction) and triplet superconducting coupling inside them; $H_{f\uparrow}$ and $H_{f\downarrow}$ originate from interband spin-flip hybridization or triplet coupling; $H_{h\uparrow}$ and $H_{h\downarrow}$ originate from interband spin-preserving hybridization and singlet coupling; the energy-shifting term such as magnetic field perpendicular to the 2D system is left out of consideration.

The equation for the self-energies of the system becomes biquadratic, allowing to uncover a band inversion at the Dirac points, in two cases. The first case is equality $|H_d| = |H_c|$ along with requirement of one type of coupling to be zero: $H_{f\uparrow} = H_{f\downarrow} = 0$ or $H_{h\uparrow} = H_{h\downarrow} = 0$. The second case is $H_c = H_d = 0$. As the magnetic field is usually a very useful instrument for creation of the higher-order topological states, the first case seems to be more promising. Moreover, in the

second case of $H_c = H_d = 0$ one can get rid of $H_{h\uparrow}$, $H_{h\downarrow}$ by unitary transformation of the basis, resulting in putting Hamiltonian (C1) in block-diagonal form and reducing the situation to the investigated earlier case with two independent subspaces. Thus, only the first case is under consideration.

Without loss of generality, we consider the situation of $H_{h\uparrow,\downarrow} = 0$ (the opposite case can be reduced to it by interchange of $|-\uparrow\rangle$, $|-,\downarrow\rangle$ order). Since the coupling terms $H_{f\sigma}$ originate from the same interactions, they are not independent. If there is only one interaction inducing $H_{f\sigma}$ it is acceptable to suppose them be equal in value and different in phase factors. Using the substitution $H_{f\sigma} = H_f e^{i\phi_{f\sigma}}$ along with $H_{c,d} = Be^{i\phi_{c,d}}$, the spectrum of the edge states will take the form

$$E^2 = \left(\sqrt{\varepsilon_p^2 + H_{fc}^2} \pm B\right)^2 + H_{fs}^2,$$
$$H_{fc} = H_f \cos\frac{\phi_c + \phi_d + \phi_{f\downarrow} - \phi_{f\uparrow}}{2},$$
$$H_{fs} = H_f \sin\frac{\phi_c + \phi_d + \phi_{f\downarrow} - \phi_{f\uparrow}}{2}. \tag{C2}$$

The result can be interpreted as follows. Without perturbations there are two Dirac cones in the edge spectrum. By adding the perturbation, the spectrum is first gapped by the H_{fc} term. Then, every branch is split into two branches and shifted by $\pm B$ generating four Dirac cones. The result is again gapped with H_{fs} term (Fig. 6). To obtain level crossing the last term is necessary. Indeed, if the last term is zero and $B \neq 0$, we obtain either gapped spectrum at any directions of boundary or gapless edge states without any effective mass sign changing. The $B = 0$ case is obviously the one, discussed earlier.

On the contrary, the case of the H_{fc} term to be zero does not exclude the level crossing. In this case, doubly degenerated initial Dirac cones are split with B (by magnetic field particularly) and then the resulting spectrum is gapped at four new Dirac points. Similarly to the situation discussed in Appendix B, H_f must be ϕ dependent and generate the same sign at all Dirac points. Consequently, the constant coupling again is not appropriate for higher-order topological phase construction. The coupling with orders of k larger than 2 is still forbidden. The only difference is that $|\lambda|$ is not equal to p at new Dirac points anymore. Unfortunately, the $(p^2 - |\lambda|^2)$ term consisting in H_f in this case has different sign in every pair of new Dirac points and there are no topological corner states again.

As a result, the consideration of full edge-state basis fails to find more simple forms of couplings to create HOTSC from two topological superconductors with inverted bands on the triangular lattice.

[1] W. A. Benalcazar, B. A. Bernevig, and T. L. Hughes, Science **357**, 61 (2017).
[2] G. E. Volovik, JETP Lett. **91**, 201 (2010).
[3] F. Zhang, C. L. Kane, and E. J. Mele, Phys. Rev. Lett. **110**, 046404 (2013).
[4] W. A. Benalcazar, J. C. Y. Teo, and T. L. Hughes, Phys. Rev. B **89**, 224503 (2014).
[5] Y. Peng, Y. Bao, and F. von Oppen, Phys. Rev. B **95**, 235143 (2017).
[6] J. Langbehn, Y. Peng, L. Trifunovic, F. von Oppen, and P. W. Brouwer, Phys. Rev. Lett. **119**, 246401 (2017).
[7] X. Zhu, Phys. Rev. B **97**, 205134 (2018).
[8] T. Liu, J. J. He, and F. Nori, Phys. Rev. B **98**, 245413 (2018).
[9] Y. Wang, M. Lin, and T. L. Hughes, Phys. Rev. B **98**, 165144 (2018).
[10] Q. Wang, C.-C. Liu, Y.-M. Lu, and F. Zhang, Phys. Rev. Lett. **121**, 186801 (2018).
[11] Z. Yan, F. Song, and Z. Wang, Phys. Rev. Lett. **121**, 096803 (2018).
[12] A. E. Hassan, F. K. Kunst, A. Moritz, G. Andler, E. Bergholtz, and M. Bourennane, Nat. Photonics **13**, 697 (2019).
[13] X.-D. Chen, W.-M. Deng, F.-L. Shi, F.-L. Zhao, M. Chen, and J.-W. Dong, Phys. Rev. Lett. **122**, 233902 (2019).
[14] X. Ni, M. Weiner, A. Alu, and B. Khanikaev, Nat. Mater. **18**, 113 (2019).
[15] H. Xue, Y. Yang, G. Liu, F. Gao, Y. Chong, and B. Zhang, Phys. Rev. Lett. **122**, 244301 (2019).
[16] C. He, S.-Y. Yu, H. Wang, H. Ge, J. Ruan, H. Zhang, M.-H. Lu, and Y.-F. Chen, Phys. Rev. Lett. **123**, 195503 (2019).
[17] Z.-X. Li, Y. Cao, X. R. Wang, and P. Yan, Phys. Rev. B **101**, 184404 (2020).
[18] Z.-X. Li, Y. Cao, X. R. Wang, and P. Yan, Phys. Rev. Applied **13**, 064058 (2020).
[19] S. Imhof, C. Berger, F. Bayer, J. Brehm, L. W. Molenkamp, T. Kiessling, F. Schindler, C. H. Lee, M. Greiter, T. Neupert, and R. Thomalem, Nat. Phys. **14**, 925 (2018).
[20] M. Serra-Garcia, R. Susstrunk, and S. D. Huber, Phys. Rev. B **99**, 020304(R) (2019).
[21] J. Bao, D. Zou, W. Zhang, W. He, H. Sun, and X. Zhang, Phys. Rev. B **100**, 201406(R) (2019).
[22] C. Nayak, S. H. Simon, A. Stern, M. Freedman, and S. DasSarma, Rev. Mod. Phys. **80**, 1083 (2008).
[23] A. C. Potter and P. A. Lee, Phys. Rev. Lett. **105**, 227003 (2010).
[24] N. Sedlmayr, J. M. Aguiar-Hualde, and C. Bena, Phys. Rev. B **93**, 155425 (2016).
[25] D. A. Ivanov, Phys. Rev. Lett. **86**, 268 (2001).
[26] J. Alicea, Y. Oreg, G. Refael, F. von Oppen, and M. P. A. Fisher, Nat. Phys. **7**, 412 (2011).
[27] Q. Cheng, J. He, and S. P. Kou, Phys. Lett. A **380**, 779 (2016).
[28] F. Harper, A. Pushp, and R. Roy, Phys. Rev. Research **1**, 033207 (2019).
[29] T. Zhou, M. C. Dartiailh, W. Mayer, J. E. Han, A. Matos-Abiague, J. Shabani, and I. Zutic, Phys. Rev. Lett. **124**, 137001 (2020).
[30] T. E. Pahomi, M. Sigrist, and A. A. Soluyanov, Phys. Rev. Research **2**, 032068(R) (2020).
[31] S. B. Zhang, W. B. Rui, A. Calzona, S. J. Choi, A. P. Schnyder, and B. Trauzettel, Phys. Rev. Research **2**, 043025 (2020).
[32] S. B. Zhang, A. Calzona, and B. Trauzettel, Phys. Rev. B **102**, 100503(R) (2020).
[33] Z. Song, Z. Fang, and C. Fang, Phys. Rev. Lett. **119**, 246402 (2017).

[34] F. Schindler, A. M. Cook, M. G. Vergniory, Z. Wang, S. S. P. Parkin, B. A. Bernevig, and T. Neupert, Sci. Adv. **4**, eaat0346 (2018).
[35] S. A. A. Ghorashi, X. Hu, T. L. Hughes, and E. Rossi, Phys. Rev. B **100**, 020509(R) (2019).
[36] A. Yoshida, Y. Otaki, R. Otaki, and T. Fukui, Phys. Rev. B **100**, 125125 (2019).
[37] J. Zou, Z. He, and G. Xu, Phys. Rev. B **100**, 235137 (2019).
[38] O. Pozo, C. Repellin, and A. G. Grushin, Phys. Rev. Lett. **123**, 247401 (2019).
[39] B. Roy, Phys. Rev. Research **1**, 032048(R) (2019).
[40] T. Mizoguchi, H. Araki, and Y. Hatsugai, J. Phys. Soc. Jpn. **88**, 104703 (2019).
[41] Y. Ren, Z. Qiao, and Q. Niu, Phys. Rev. Lett. **124**, 166804 (2020).
[42] S. Qian, C.-C. Liu, and Y. Yao, Phys. Rev. B **104**, 245427 (2021).
[43] Y.-J. Wu, J. Hou, Y.-M. Li, X.-W. Luo, X. Shi, and C. Zhang, Phys. Rev. Lett. **124**, 227001 (2020).
[44] S. Ikegaya, W. B. Rui, D. Manske, and A. P. Schnyder, Phys. Rev. Research **3**, 023007 (2021).
[45] E. Khalaf, W. A. Benalcazar, T. L. Hughes, and R. Queiroz, Phys. Rev. Research **3**, 013239 (2021).
[46] M. Ezawa, Phys. Rev. Lett. **120**, 026801 (2018).
[47] S. N. Kempkes, M. R. Slot, J. J. van den Broeke, P. Capoid, W. A. Benalcazar, D. Vanmaekelbergh, D. Cercioux, I. Swart, and C. M. Smith, Nat. Mater. **18**, 1292 (2019).
[48] A. Sil and A. K. Ghosh, J. Phys: Condens. Matter **32**, 205601 (2020).
[49] W. P. Su, J. R. Schrieffer, and A. J. Heeger, Phys. Rev. Lett. **42**, 1698 (1979).
[50] G. van Miert and C. Ortix, Quantum Mater. **5**, 63 (2020).
[51] E. Roberts, J. Behrends, and B. Beri, Phys. Rev. B **101**, 155133 (2020).
[52] M. Jung, Y. Yu, and G. Shvets, Phys. Rev. B **104**, 195437 (2021).
[53] A. D. Fedoseev, J. Phys.: Condens. Matter **32**, 405302 (2020).
[54] W. A. Benalcazar, T. Li, and T. L. Hughes, Phys. Rev. B **99**, 245151 (2019).
[55] F. Schindler, Z. Wang, M. G. Vergniory, A. M. Cook, A. Murani, S. Sengupta, A. Y. Kasumov, R. Deblock, S. Jeon, I. Drozdov, H. Bouchiat, S. Gueron, A. Yazdani, B. A. Bernevig, and T. Neupert, Nat. Phys. **14**, 918 (2018).
[56] L. Aggarwal, P. Zhu, T. L. Hughes, and V. Madhavan, Nat. Commun. **12**, 4420 (2021).
[57] I. K. Drozdov, A. Alexandradinata, S. Jeon, S. Nadj-Perge, H. Ji, R. J. Cava, B. A. Bernevig, and A. Yazdani, Nat. Phys. **10**, 664 (2014).
[58] Z. Wang, B. J. Wieder, J. Li, B. Yan, and B. A. Bernevig, Phys. Rev. Lett. **123**, 186401 (2019).
[59] M. Ezawa, Sci. Rep. **9**, 5286 (2019).
[60] S. Qian, G.-B. Liu, C.-C. Liu, and Y. Yao, Phys. Rev. B **105**, 045417 (2022).
[61] T. Senthil, J. B. Marston, and M. P. A. Fisher, Phys. Rev. B **60**, 4245 (1999).
[62] T. Chern, AIP Adv. **6**, 085211 (2016).
[63] A. Altland and M. R. Zirnbauer, Phys. Rev. B **55**, 1142 (1997).
[64] C.-K. Chiu, J. C. Y. Teo, A. P. Schnyder, and S. Ryu, Rev. Mod. Phys. **88**, 035005 (2016).
[65] M. Ezawa, Phys. Rev. B **102**, 121405(R) (2020).
[66] E. Khalaf, Phys. Rev. B **97**, 205136 (2018).
[67] A. D. Fedoseev, J. Phys.: Condens. Matter **32**, 215301 (2020).
[68] A. M. Black-Schaffer and C. Honerkamp, J. Phys.: Condens. Matter **26**, 423201 (2014).